Use of Geosynthetics for Reinforcing/Stabilizing Unpaved Roads under Full-Scale Truck Axle Loads

Xiaochao Tang[1], Ph. D., Murad Abu-Farsakh[2], Ph. D., P. E., Shadi Hanandeh[3] and Qiming Chen[4] , Ph. D., P. E.

[1]Assistant Professor, Department of Civil and Environmental Engineering, Widener University, One University Place, Chester, PA 19013; xtang@widener.edu
[2]Research Professor, Louisiana Transportation Research Center, Louisiana State University, 4101 Gourrier Ave., Baton Rouge, LA 70808; cefars@lsu.edu
[3]Graduate Research Assistant, Department of Civil and Environmental Engineering, Louisiana State University, Baton Rouge, LA 70808; shanan1@tigers.lsu.edu
[4]Research Associate, Louisiana Transportation Research Center, Louisiana State University, 4101 Gourrier Ave., Baton Rouge, LA 70808; qchen1@tigers.lsu.edu

ABSTRACT: The significant impact of the truck traffic associated with the shale energy developments on local roads, including many unpaved gravel roads has been a pressing issue while the regional economy benefits from the recent shale gas boom. In many cases, roads had to be reconstructed over a soft soil subgrade treated and stabilized by cement or lime. As an alternative, geosynthetics offer a potentially more cost effective solution for reinforcing/stabilizing roads on soft soil subgrade. This paper presents a study using a full-scale accelerated traffic load testing to evaluate two recently emerged geosynthetic products, a triaxial geogrid and a high-strength woven geotextile in unpaved roads built over soft soil subgrade. A total of six full-scale test sections were constructed, among which two sections were reinforced by one and two layers of triaxial geogrids, respectively; while high strength geotextiles were used to reinforce two of the other sections with different aggregate layer thicknesses. The rest of the two sections were left as control sections, of which one section was constructed over 30-cm thick sand embankment. The test sections were subjected to a full-scale moving wheel load applied by the Accelerated Loading Facility (ALF). A variety of instrumentations were used to measure the load-associated and the environment-associated responses and performance of the unpaved test sections. Results of the full-scale testing on the unpaved test sections demonstrate the benefits of geosynthetics in reducing the permanent deformation/rutting.

INTRODUCTION

In recent years, there has been a boom of shale gas energy development in some parts of the country. While the regional economy benefits from the shale gas energy, the significant impact of shale gas development-related activities on local roads has been a

pressing issue. The truck traffic associated with the shale gas development typically starts with the movement of the drill rig and equipment, which requires approximately 20 oversize and overweight truck permits (Kuhn, 2006). There is also truck traffic related to construction activities such as the transportation of construction equipment and materials for constructing the pad site and access road. Among all of the shale gas development-related activities, hydraulic fracturing generates the most truck traffic, which involves moving about 5 million gallons of water and delivering about 2500 tons of sands for a typical deep shale gas well (Cheasapeak Energy, 2012; Gannett Fleming, 2011).

It is often difficult to estimate and quantify the impacts on local roads from the truck traffic associated with the shale energy development since it requires detailed information such as the road structure and materials, truck traffic characteristics, and climate conditions of the region (Mason et al., 1982; Quiroga et al., 2012). Nonetheless, a theoretical study on highway roads has indicated that the shale gas development truck traffic could cause additional damage to the highway roads by a rate as high as 13% and a reduction of highway road service life by 29% (Banerjee et al., 2012). Particularly, in states such as Pennsylvania and New York where freeze-thaw cycles are frequently encountered in road subgrades, the heavy hauling truck load associated with the shale gas development has caused significant challenges to road maintenance and rehabilitation, especially during the spring season with the weakened soil subgrade. In many cases, roads had to be reconstructed over a stabilized subgrade treated by stabilizers such as cement and lime. As a mechanical stabilization of soil, geosynthetics offer an alternative solution for reinforcing/stabilizing roads built on soft soil subgrade.

Numerous studies have shown that geosynthetics provide benefits in roadway structures by either extending the roads' service life or reducing the structural layer thickness, especially the aggregate layer, with an equivalent performance (Barksdale et al., 1989; Al-Qadi et al., 1994; Perkins et al, 2004; Tang et al., 2008; Abu-Farsakh et al., 2012). Aimed to evaluate two recently emerged geosynthetic products, a triaxial geogrid and a high-strength woven geotextile, a full-scale accelerated pavement testing was conducted on a total of six test lane sections constructed over soft subgrade soil. Each section was instrumented by a variety of sensors to measure the critical responses and performance and the environmental factors that may affect the performance of test sections. The response and performance measurements are intended to be used to calibrate and/or develop ME models that can account for the effects of geosynthetics in pavement design.

TESTING PROGRAM

Full-Scale Test Section

A total of six test lane sections were constructed over soft soil foundation at an outdoor site located at the Pavement Research Facility (PRF) of Louisiana Department of Transportation and Development (LA DOTD) in Port Allen, LA. The dimension of each test section is 24 m (80 ft) long and 4 m (13 ft) wide. Fig. 1-a shows the cross sections of the six test lane sections, while Fig. 1-b shows a photo during the

construction of test sections. Section 1 and Section 4 are the control sections that were constructed without geosynthetic reinforcements, of which Section 1 was constructed over an embankment of 30 cm thick sand wrapped by nonwoven geotextiles. Section 4 is a typical control section without geosynthetics. Section 2 and Section 3 were reinforced/stabilized by the triaxial geogrid, GG, placed at the aggregate base - subgrade interface. An additional layer of geogrid, GG, reinforcement was also installed at the upper one-third of the aggregate base layer thickness in Section 2. The high strength geotextiles, GT, were used to reinforce/stabilize Section 5 and Section 6 with different aggregate layer thicknesses.

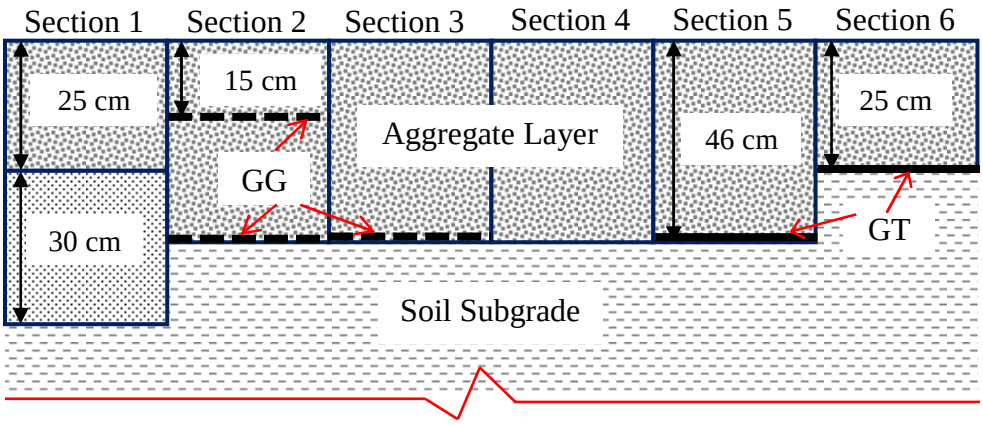

(a) Cross section of the test sections

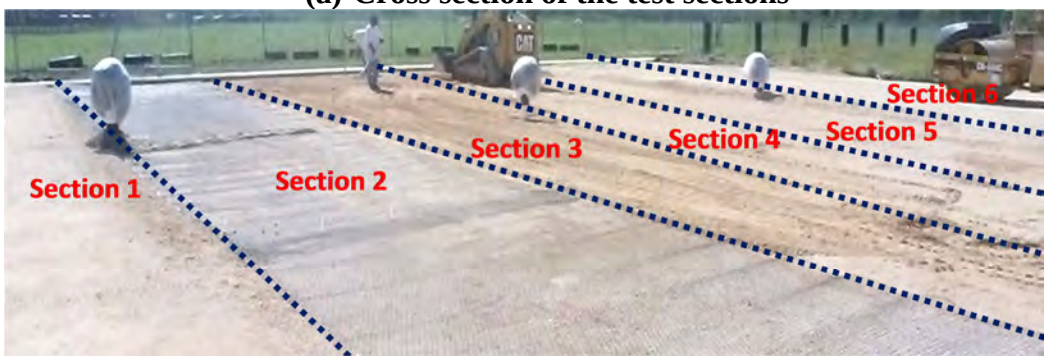

(b) Construction of sections

FIG. 1. Test sections

The native subgrade soil in this study is classified as heavy clay (CH) per Unified Soil Classification System (USCS) or A-7-6 according to the American Association of State Highway and Transportation (AASHTO) classification system. The soil has a plasticity index, PI, of 55% with 96.6% passing the #200 sieve. The subgrade soil has an optimum moisture content of 29.5% and a maximum dry density of 1305 kg/m^3, according to the Standard proctor test. The aggregate used in this study is a dense-graded crushed limestone classified as GW or A-1-a. A modified Proctor test of the aggregate yields an optimum moisture content of 9.4% and a maximum dry density of 2066 kg/m^3.

Two recently emerged geosynthetic products, a triaxial geogrid and a high-strength woven geotextile, are selected for this study and are herein designated as GG and GT.

The triaxial geogrid was made by means of punching and drawing polypropylene (PP) sheets. The geotextile was made from high-tenacity polypropylene filaments that are formed into weaves.

Instrumentation

The test sections were instrumented by a variety of sensors to measure the load – and environment – associated pavement responses and performance. Spring-loaded LVDTs (RDP DCTH2000A) were customized to measure the total deformation of the subgrade. A thin yet rigid disk with a diameter of 5 cm (2 in) was attached onto the contact tip of the spring-loaded LVDT to provide sufficient contact area with the soil (Fig. 2-a). Potentiometers (Honeywell MLT-38000201) were customized to measure the strain at the mid-height of the aggregate layer. The potentiometer has a maximum travel distance of 25.4 mm (1 in). Two circular end plates with diameters of 5 cm were attached onto the potentiometer (Fig. 2-b).

(a) **(b)**

FIG. 2. Instrumentation sensors for the test lane sections: (a) LVDT; (b) customized potentiometer

The geosynthetics were instrumented with foil strain gauges installed in pairs on opposite sides of the geosynthetic. Other instruments including thermocouples to measure temperature variation and time-domain reflectometers (TDR) for monitoring the moisture contents were installed. Also, earth pressure cells (Geokon 3500) and piezometers (Geokon 3400) were installed at the top of the subgrade to measure the total vertical stress and possible excess pore water pressure generated by the cyclic wheel load.

Full-Scale Accelerated Testing

A full-scale accelerated load facility (ALF) was used to apply cyclic moving wheel loads on test lane sections. Fig. 3 shows a picture of the ALF with an insert of the dual-wheel assembly. ALF is a testing device that applies unidirectional trafficking to the test sections with a nominal speed of 16.8 km/h (10.5 mph) or 350 passes per hour. ALF has a due-tire axle consisting of two Michelin XZE-model truck tires and applies a 43.4-kN (9,750-lb) axle load, approximately representing half of the standard axle

load, the 80-kN (18-kip) single-axle load. ALF has the capacity of applying a normally- distributed wander covering a transverse distance of 76 cm (30 in) to simulate live traffic pattern. The wheel path generated by ALF is about 12 m (40 ft) long.

At the end of the testing, a total of 2000 passes were applied to the sections with geosynthetic reinforcements, while only 400 passes were applied to the two control sections. Using a laser profilometer, the transverse surface profile of the test sections were measured at selected intervals of load repetitions at 8 different locations along the wheel path.

FIG. 3. The accelerated load facility (ALF) with an insert of the dual-wheel assembly.

RESULTS AND ANALYSIS

Surface Rutting

Fig. 4-a presents the accumulation of the surface rutting/total permanent deformation along with the number of wheel passes for the six test lane sections. The total permanent deformation for each test lane section shown in Fig. 4-a is the average of the measurements taken at the different locations along the wheel path in each section. The control sections, Section 1 and Section 4, exhibited significantly greater total permanent deformation than the reinforced sections under the same number of wheel load passes, indicating the benefits of geosynthetics mobilization in reducing permanent deformation in unpaved roads built over soft soil subgrade.

Between Sections 2 and 3, Section 2 reinforced with two layers of geogrids showed less permanent deformation at the end of the testing. Furthermore, there is less deformation at the early stage of the traffic in Section 2, which is most likely due to the mobilization of the geogrid layer installed at the upper one-third of the aggregate layer in Section 2. The two control sections, Section 1 and Section 4 showed almost similar performance in terms of total permanent deformation.

Compared to the test sections (Sections 2 and 3) that are reinforced with triaxial geogrids (GG), the test sections (Sections 5 and 6) with high-strength geotextile (GT), showed less permanent deformations. It should be pointed out that, in addition to the presence of geosynthetics or geosynthetic types, there are other factors that can affect the performance of the test sections in terms of resisting the surface rutting. The deformations needed to mobilize the triaxial geogrids might be different than the

high-strength geotextile. The variations in construction such as degree of compaction may significantly affect the pavement performance. Although efforts were made to ensure consistent or similar testing conditions for all test sections, the possible change of the subgrade soil and aggregate layer conditions throughout the testing process may affect the sections' stiffness and strength, and thus their performance. In-situ tests conducted after the accelerated load testing, to be presented later, showed that the dry density and modulus at testing were higher for Section 5 and Section 6, which may attributable to that Section 5 and Section 6 had a less permanent deformation.

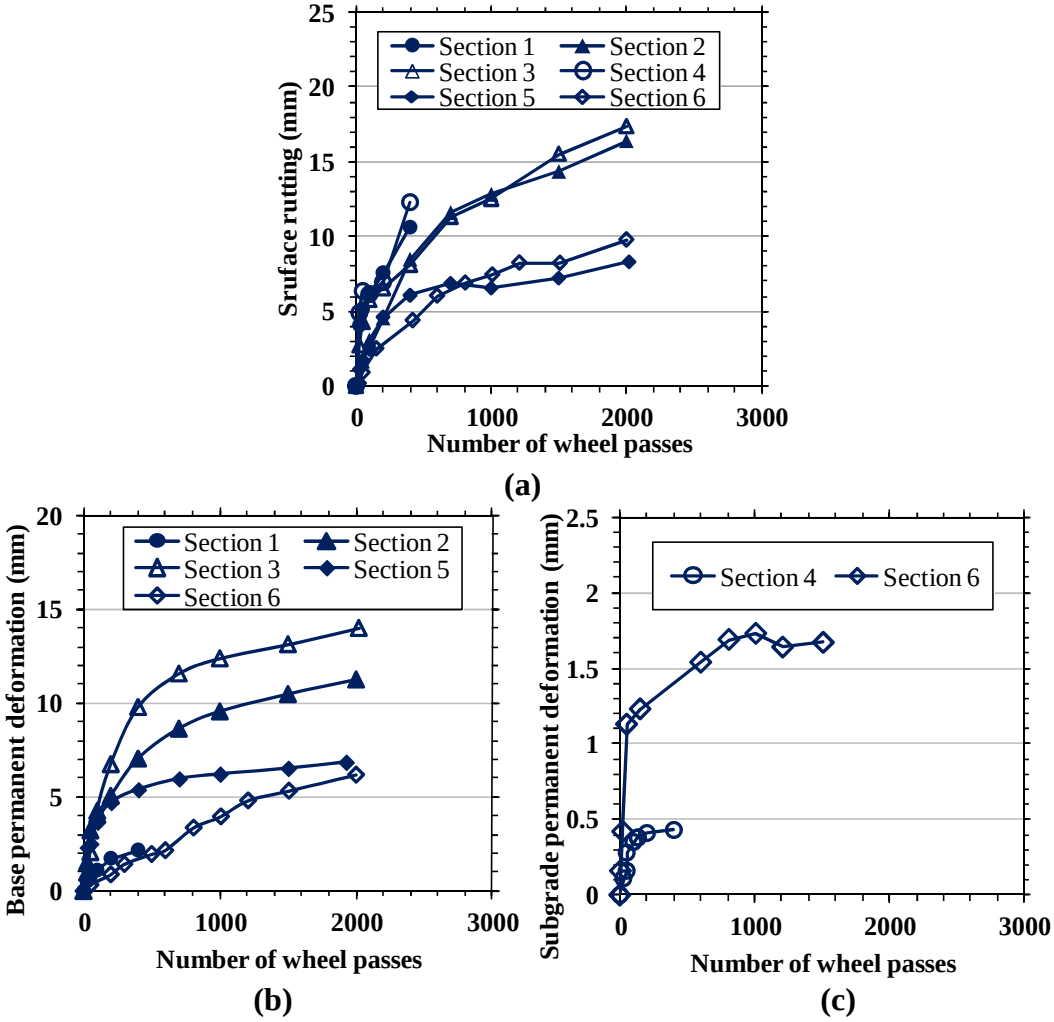

FIG. 4. Accumulated permanent deformation: (a) on the surface; (b) in aggregate layer; (c) in subgrade.

Permanent Deformation in Aggregate Layer and Subgrade

Two customized potentiometers were installed at the mid-height of the aggregate layer for each test section. Measurements from the potentiometer were relative distances between its two end plates. The change of the distance is converted into the compressive strain that is subsequently used to estimate the deformation of the

aggregate layer by multiplying with the overall thickness of the aggregate layer. The use of the potentiometer measurements for estimating the aggregate layer deformation is based on the assumption that the compressive strain of the aggregate layer is uniformly distributed and represented by the mid-height compressive strain. Fig. 4-b presents the derived permanent deformation of the aggregate layer for each test section except for Section 4 due to the potentiometer malfunction.

Sections 2 and 3 reinforced by GG exhibited more permanent deformation in the aggregate layer than Sections 5 and 6 reinforced with GT. Compared to Section 3, Section 2 with two layers of geogrids showed significantly less aggregate layer deformation. Unlike other test sections, Section 6 showed a nearly linear increase of the aggregate layer permanent deformation. Although Section 1 showed a higher total permanent deformation at the same number of wheel passes, the aggregate layer deformation in Section 1 is relatively smaller, indicating that the underlying sand embankment may significantly contribute to the overall permanent deformation in Section 1.

The LVDTs were mounted in a steel rod, which had one end relatively fixed to a great depth of the soil foundation. Therefore, the permanent deformation measured by LVDTs represented the overall deformation of the entire subgrade layer. Fig. 4-c shows the accumulation of subgrade permanent deformation along with the number of wheel passes for Section 4 and Section 6. LVDTs in other test sections were out of order during the accelerated pavement testing. As can be seen in Fig. 4-c, the control section (Section 4) has a significantly less deformation than Section 6 reinforced by the high-strength geotextile. This is likely due to the fact that the aggregate layer of Section 4 is 21 cm (8 in) thicker than that of Section 6, suggesting that the additional 21 cm (8 in) aggregate layer provides more protection to the subgrade than the high-strength geotextile layer does.

The total surface permanent deformation or surface rutting for each test section consists of permanent deformation in the aggregate layer and the subgrade permanent deformation. It is noted that the majority of the total permanent deformation is generally attributed to the permanent deformation in the aggregate layer. The load-induced permanent deformation is usually a result of material densification, shear-related deformation, or a combination of both, which can occur in any layer of the pavement system. Measurements of aggregate layer deformation demonstrate that the aggregate layer has the greatest relative layer contributions to the total permanent deformation.

Strain Developed in Geosynthetics

Foil strain gauges were installed on opposite surfaces at each location to measure tensile strains developed in geosynthetics with the repetitions of the traffic load. The measurements from strain gauges installed on opposite surfaces should be averaged to account for the flexural bending effects (Tang et al., 2013).

Fig. 5 shows the geosynthetic tensile strains measured at the centerline of the test sections. No reliable results from strain measurements were obtained in Section 5 due to the loss of strain gauges. Among the geosynthetics installed at the subgrade - aggregate base layer interface, the geotextile in Section 6 showed higher tensile strain

at the end of the loading. Between the two layers of geogrids in Section 2, the geogrid installed at the upper one-third of the aggregate layer developed the tensile strains that are more than twice as the geogrid installed at the subgrade-aggregate layer interface. Overall, Fig. 5 demonstrates that the geosynthetics were all mobilized at the end of the accelerated loading.

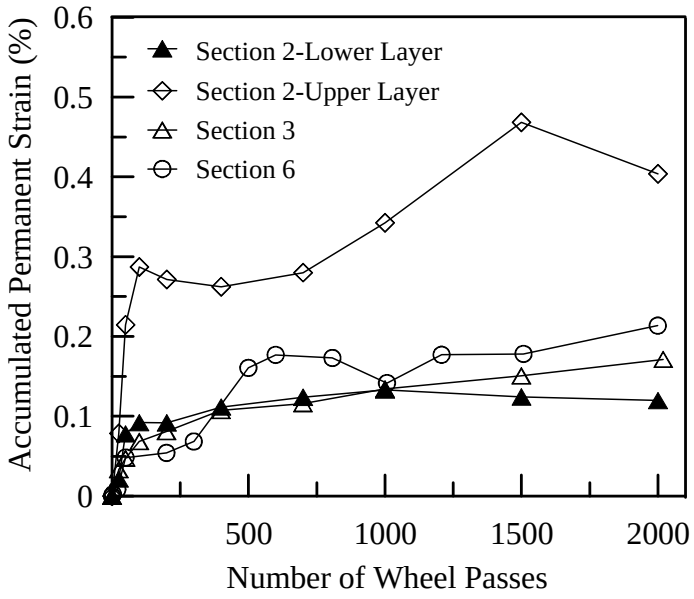

FIG. 5. Strains developed in geosynthetics at the center of test sections.

In-Situ Testing

In-situ tests were conducted upon the completion of accelerated testing on the aggregate layer along two locations: inside and 0.9 m (3 ft) outside the wheel path. The purpose of these tests is to characterize the respective site conditions before and after the traffic loading. For each test section, the in-situ testing was conducted at a minimum of five locations inside and outside wheel path, respectively. Table 1 presents the in-situ dry density and moisture content measured by the nuclear gauge. Section 6 showed the highest dry density in the aggregate layer followed by Section 3. Except for Section 4, there is a noticeable increase of dry density for locations inside the wheel path compared to locations outside the wheel path, indicating a further compaction of the aggregate layer from the repetitive wheel load.

Table 2 lists the aggregate layer moduli tested by different devices at locations inside and outside the wheel path. For the moduli tested by light-weight deflectometer (LWD) and GeoGauge, no significant difference was observed between the locations inside and outside the wheel path. Between the reinforced sections and comparable control section, e.g. sections 2, 3, and 4, no evident increase of resilient modulus was observed due to the geosynthetic reinforcements, which is in agreement with other study (Tang et al., 2014). Dynamic cone penetrometer (DCP) tests were conducted on the aggregate layer and results were converted into moduli based on a correlation model (Mohammad et al., 2008). The aggregate base moduli showed an overall increase for

locations inside the wheel path, which reflects the change of dry density measured by the nuclear gauge (Table 1). Additionally, among the different test sections, the DCP testing results showed a good correlation with the in-situ dry density. This suggests that measurements from the nuclear gauge density and DCP may be more reliable. Section 6 showed a higher DCP-derived aggregate layer modulus compared to other sections, which contributes to that Section 6 had relatively less surface rutting despite its thinner aggregate layer. Table 3 lists the subgrade modulus value from DCP tests. It can be seen that Section 6 had a higher in-situ subgrade modulus, which is also attributable to the less rutting observed in Section 6.

Table 1. Dry density and moisture content of the aggregate layer

Test Sections	Dry Density (kg/m^3)				Moisture Content (%)			
	Outside wheel path		Inside wheel path		Outside wheel path		Inside wheel path	
	Avg.	Stdv.	Avg.	Stdv.	Avg.	Stdv.	Avg.	Stdv.
1	1986.0	28.9	2017.0	19.3	6.1	0.3	5.8	0.3
2	1988.3	62.0	2002.7	33.8	5.7	0.8	6.0	0.6
3	2012.9	30.8	2038.1	21.0	5.6	0.2	6.3	0.4
4	1985.2	38.0	1949.0	33.5	5.9	0.3	5.5	0.4
5	2000.9	37.9	2036.8	26.4	7.6	0.3	7.1	0.4
6	2015.6	40.1	2040.7	30.3	5.5	0.2	5.3	0.2

Table 2. Resilient modulus for aggregate layer moduli outside and inside wheel path from LWD, GeoGauge, and DCP testing

Test Sections	LWD (MPa)				GeoGauge (MPa)				DCP (MPa)			
	Outside wheel path		Inside wheel path		Outside wheel path		Inside wheel path		Outside wheel path		Inside wheel path	
	Avg.	Stdv.	Avg.	Stdv.	Avg.	Stdv.	Avg.	Stdv.	Avg.	Stdv.	Avg.	Stdv.
1	51.8	2.8	51.7	3.4	70.5	12.0	72.2	4.8	37.4	0.9	39.6	0.5
2	49.6	1.8	50.7	3.6	71.5	43.9	68.3	16.9	36.0	1.1	38.8	0.9
3	52.0	15.1	50.2	14.9	75.8	26.4	72.4	11.4	38.7	1.6	40.9	0.5
4	50.6	4.3	49.6	1.3	72.5	35.4	69.2	19.4	34.9	0.3	37.0	0.7
5	52.4	4.4	51.2	3.4	75.4	22.9	72.1	24.4	38.0	1.0	41.2	1.7
6	45.8	18.7	45.3	11.1	77.7	38.3	69.9	13.1	41.1	1.8	41.9	2.0

Table 3. Subgrade modulus derived from DCP tests, units in MPa

Test Section	Inside Wheel Path		Outside Wheel Path	
	Avg.	Stdv.	Avg.	Stdv.
1	23.5	2.1	21.2	0.7
2	22.0	0.6	21.1	0.4
3	23.5	1.6	21.5	0.9
4	20.1	1.7	21.9	0.7
5	22.6	0.7	20.9	1.0
6	24.6	0.8	24.7	1.0

SUMMARY AND CONCLUSIONS

The truck traffic associated with the shale gas development has caused significant challenges to the maintenance and rehabilitation of local roads, including many unpaved gravel roads. Geosynthetics offer an alternative for reinforcing/stabilizing unpaved roads built over soft soil subgrade. A full-scale accelerated load testing was conducted to evaluate the benefits of using two recently emerged geosynthetics, a triaxial geogrid and a high-strength woven geotextile to reinforce/stabilize unpaved roads. A total of six test lane sections were constructed over soft subgrade soil, and were extensively instrumented to measure the critical pavement responses and performance. The findings and conclusions are summarized as follows:

1) Results of the full-scale accelerated load testing demonstrated the benefits of both geosynthetic products in significantly reducing the total permanent deformation/surface rutting of unpaved test sections. Likely due to the stiffer subgrade and aggregate layer, the two test sections with geotextile showed less permanent deformation than the sections with geogrids.
2) An important finding is that the majority of the surface permanent deformation was attributed to the aggregate layer, instead of the soft subgrade layer. The deformation in the aggregate layer is most likely due to further compaction and densification of the layer. However, Section 1 with a sand embankment showed less deformation in the aggregate layer, indicating that the sand embankment may contribute to the majority of the permanent deformation in Section 1.
3) Measurements from the strain gauges demonstrate that the geosynthetics were mobilized during the accelerated testing. In general, the permanent strain developed in the geosynthetic was around 0.2% at the end of the accelerated load testing. The geogrid installed at the upper one-third of the aggregate layer in Section 2 showed twice more tensile strains than that of the geogrid installed at the subgrade-aggregate layer interface in Section 2.
4) Extensive in-situ tests using various devices were conducted to characterize the site conditions before and after the accelerated load testing. No appreciable change of aggregate layer moduli before and after the accelerated load testing was observed from the non-destructive LWD and GeoGauge tests. The more reliable intrusive measurements by the nuclear gauge and DCP demonstrate that Section 6 had a relatively higher modulus in the aggregate layer and subgrade than other sections, which may be attributable to that Section 6 has relatively less rutting despite its thinner aggregate layer.

ACKNOWLEDGMENTS

The authors would like to acknowledge the financial support provided by the Louisiana Department of Transportation and Development (LA DOTD), Tensar International, and Mirifi TenCate.

REFERENCES

Abu-Farsakh, M. Y., Souci, G., Voyiadjis, G. Z., and Chen, Q. (2012). "Evaluation of Factors Affecting the Performance of Geogrid-Reinforced Granular Aggregate layer Material Using Repeated Load Triaxial Tests." *Journal of Materials in Civil Engineering*, 24(1): 72-83.

Al-Qadi, I.L, Brandon, T.L., Valentine, R.J., Lacina, B.A., and Smith, T.E. (1994). "Laboratory Evaluation of Geosynthetic-Reinforced Pavement Sections." *Transportation Research Record 1439*, Transportation Research Board, National Research Council, Washington D.C., 25-31.

Banerjee, A., Prozzi, J. P., Prozzi, J. A. (2012). "Evaluating the Effect of Natural Gas Developments on Highways: Texas Case Study" *Transportation Research Record 2282*, Transportation Research Board, Washington, D.C., 49-56.

Barksdale, R.D., Brown, S. F., and Chan, F. (1989). "Potential Benefits of Geosynthetics in Flexible Pavement Systems." *National Cooperative Highway Research Program Report No. 315*, Transportation Research Board, National Research Council, Washington D.C.

Chesapeake Energy (2012). *Water Use in Deep Shale Gas Exploration*. Chesapeake Energy Fact Sheet, May 2012.

Gannett Fleming (2011). *Marcellus Shale Freight Transportation Study*. Northern Tier Regional Planning & Development Commission.

Kuhn, D. (2006). *Highway Freight Traffic Associated with the Development of Oil and Gas Wells*. Utah Department of Transportation, Salt Lake City, Utah.

Mason, J. M., Metyko, M. J., and Rowan, N. J. (1982). The Effects of Oil Field Development on Rural Highways. *Report No. TTI-2-10-81-229-1*. Texas Transportation Institute, Texas A&M University System, College Station, TX.

Mohammad, L. N., Herath, A., Gudishala, R., Nazzal, M. D., Abu-Farsakh, M. Y., and Alshibli, K. (2008). Development of Models to Estimate the Subgrade and Subaggregate layer Layers' Resilient Modulus from In situ Devices Test Results for Construction Control. *Report No. 406*, Louisiana Transportation Research Center, Baton Rouge, LA 70808.

Perkins, S. S., Christopher, B. R., Cuelho, E.L., Eiksund, G. R. (2004). "Development of Design Methods for Geosynthetic Reinforced Flexible Pavements." *Report No. DTFH61-01-X-00068*, U.S. Department of Transportation, Federal Highway Administration, Washington, D.C.

Quiroga, C., Fernando, E., and Oh, J. (2012). Energy Developments and the Transportation Infrastructure in Texas: Impacts and Strategies. *FHWA/TX-12/0-6498-1*, Texas Department of Transportation, Research and Technology Implementation Office, Austin, TX.

Tang, X., Chehab, G.R., and Palomino, A.M. (2008). "Evaluation of Geogrids for Stabilizing Weak Pavement Subgrade." *International Journal of Pavement Engineering*, Vol. 9 (5): 413-429.

Tang, X., Palomino, A. M., and Stoffels, S. M. (2013). "Reinforcement Tensile Behavior Under Cyclic Moving Wheel Loads." *Transportation Research Record 2363*, Transportation Research Board, Washington, D.C., 113-121.

Tang, X., Stoffels, S. M., and Palomino, A. M. (2014). "Resilient and Permanent

Deformation Characteristics of Unbound Pavement Layers Modified by Geogrids." *Transportation Research Record 2369*, Transportation Research Board, Washington, D.C., 3-10.